NANO LETTERS

2007
Vol. 7, No. 8
2499−2505

Electrostatic Potential in a Bent Piezoelectric Nanowire. The Fundamental Theory of Nanogenerator and Nanopiezotronics

Yifan Gao and Zhong Lin Wang*

School of Materials Science and Engineering, Georgia Institute of Technology, Atlanta, Georgia 30332-0245

Received June 2, 2007

ABSTRACT

We have applied the perturbation theory for calculating the piezoelectric potential distribution in a nanowire (NW) as pushed by a lateral force at the tip. The analytical solution given under the first-order approximation produces a result that is within 6% from the full numerically calculated result using the finite element method. The calculation shows that the piezoelectric potential in the NW almost does not depend on the *z*-coordinate along the NW unless very close to the two ends, meaning that the NW can be approximately taken as a "parallel plated capacitor". This is entirely consistent to the model established for nanopiezotronics, in which the potential drop across the nanowire serves as the gate voltage for the piezoelectric field effect transistor. The maximum potential at the surface of the NW is directly proportional to the lateral displacement of the NW and inversely proportional to the cube of its length-to-diameter aspect ratio. The magnitude of piezoelectric potential for a NW of diameter 50 nm and length 600 nm is ∼0.3 V. This voltage is much larger than the thermal voltage (∼25 mV) and is high enough to drive the metal–semiconductor Schottky diode at the interface between atomic force microscope tip and the ZnO NW, as assumed in our original mechanism for the nanogenerators.

Developing novel technologies for wireless nanodevices and nanosystems is of critical importance for applications in biomedical sensing, environmental monitoring, and even personal electronics. Miniaturization of a power package and self-powering of these tiny devices are some key challenges for their applications. Various approaches have been developed for harvesting energy from the environment based on approaches such as thermoelectricity and piezoelectricity. Innovative nanotechnologies are being developed for converting mechanical energy (such as body movement, muscle stretching), vibration energy (such as acoustic/ultrasonic wave), and hydraulic energy (such as body fluid and blood flow) into electric energy that will be used to power nanodevices that operate at low power.

Recently, using piezoelectric ZnO nanowire (NW) arrays, a novel approach has been demonstrated for converting nanoscale mechanical energy into electric energy.[1−3] The single nanowire nanogenerator (NG) relies on the bending of a NW by a conductive atomic force microscope (AFM) tip, which transfers the displacement energy from the tip to the elastic bending energy of the NW. The coupled piezoelectric and semiconducting properties of the NW perform a charge creation, accumulation, and discharge process. Most recently, this approach has been extensively developed to produce continuous direct-current output with the use of aligned NWs that were covered by a zigzag top electrode, and the nanogenerator was driven by ultrasonic wave, establishing the platform of producing usable power output for nanodevices by harvesting energy from the environment.[4] Furthermore, based on the coupled piezoelectric and semiconducting properties of the NW, a new field of nanopiezotronics has been created,[5,6] which is the basis for fabricating piezoelectric field effect transistors,[7] piezoelectric diode,[8] piezoelectric force/humidity/chemical sensors,[9] and more.

The theoretical background for the nanogenerator and nanopiezotronics is based on a voltage drop created across the cross section of the NW when it is laterally deflected, with the tensile side surface in positive voltage and compressive side in negative voltage.[1,5] It is essential to quantitatively calculate and even develop analytical equations that can give a direct calculation of the voltage at the two side surfaces of the NW, which is important to calculating the efficiency of the nanogenerator and the operation voltage of the nanopiezotronics. In the literature, numerous theories for one-dimensional (1D) nanostructure piezoelectricity have been proposed, including first-principles calculations,[10,11] molecular dynamics (MD) simulations,[12] and continuum models.[13] However, first-principle theory and MD simulation are difficult to be implemented to the nanopiezotronics system

* Corresponding author. zlwang@gatech.edu.

10.1021/nl071310j CCC: $37.00
Published on Web 07/24/2007

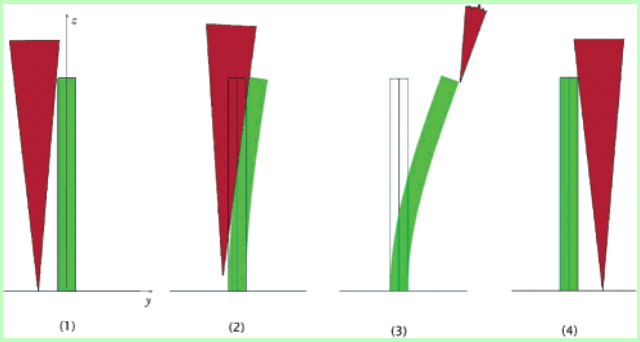

Figure 1. The typical configuration of a ZnO nanogenerator. When pushed by an AFM tip, mechanical deflection gives rise to an electrical field, the power of which can be released. The pushing force increases from (1) to (3), until (4) the wire is released.

(the typical dimension of which is ~50 nm in diameter and ~2 μm in length) due to the huge number of atoms. The continuum model proposed by Michalski et al. is relevant in that it gives a criterion to distinguish between a mechanically dominated regime and an electrostatically dominated regime. But since their theory is 1D in nature, it is best suited to elongation/torsion problems, while piezotronics systems usually involve lateral bending thus strain profile across the NW cross section is important. In this paper we propose a continuum model for the electrostatic potential in a laterally bent NW. A perturbation technique is introduced to solve the coupled differential equations, and the derived analytical equation gives a result that is within 6% of that received from full numerical calculation. The theory directly establishes the physical basis of nanopiezotronics and nanogenerator as proposed previously.[1,5]

1. Analytical Solution via Perturbation Theory.

1.1. System Setup and Governing Equations. The typical setup of a vertical piezoelectric nanowire nanogenerator is shown in Figure 1. The NW is pushed laterally by an AFM tip. Piezoelectric potential/field is created by the NW. Our theoretical objective is to derive the relationship between the potential distribution in the NW and the dimensionality of the NW and magnitude of the applied force at the tip. For this purpose, we start from the governing equations for a static piezoelectric material, which are three sets: mechanical equilibrium equation (eq 1), constitutive equation (eq 2), geometrical compatibility equation (eq 3), and Gauss equation of electric field (eq 4). The mechanical equilibrium condition when there is no body force $\vec{f}_e^{(b)} = 0$ acting on the nanowire is

$$\nabla \cdot \sigma = \vec{f}_e^{(b)} = 0 \tag{1}$$

where σ is the stress tensor, which is related to strain ϵ, electric field $\vec{E}$, and electric displacement $\vec{D}$ by constitutive equations

$$\begin{cases} \sigma_p = c_{pq}\epsilon_q - e_{kp}E_k \\ D_i = e_{iq}\epsilon_q + \kappa_{ik}E_k \end{cases} \tag{2}$$

Here c_{pq} is the linear elastic constant, e_{kp} is the linear piezoelectric coefficient, and κ_{ik} is the dielectric constant. It must be pointed out that eq 2 does not contain the contribution from the spontaneous polarization introduced by the polar charge on the $\pm$(0001) polar surfaces,[14] which are the top and bottom ends of the NW, respectively. The validity of this approximation will be elaborated later. To keep the notation compact, the so-called Voigt (or Nye) two-index notation[15] is used. By considering the C_{6v} symmetry of a ZnO crystal (with wurtzite structure), c_{pq}, e_{kp}, and κ_{ik} can be written as

$$c_{pq} = \begin{pmatrix} c_{11} & c_{12} & c_{13} & 0 & 0 & 0 \\ c_{12} & c_{11} & c_{13} & 0 & 0 & 0 \\ c_{13} & c_{13} & c_{33} & 0 & 0 & 0 \\ 0 & 0 & 0 & c_{44} & 0 & 0 \\ 0 & 0 & 0 & 0 & c_{44} & 0 \\ 0 & 0 & 0 & 0 & 0 & \dfrac{(c_{11}-c_{12})}{2} \end{pmatrix} \tag{2.1}$$

$$e_{kp} = \begin{pmatrix} 0 & 0 & 0 & 0 & e_{15} & 0 \\ 0 & 0 & 0 & e_{15} & 0 & 0 \\ e_{31} & e_{31} & e_{33} & 0 & 0 & 0 \end{pmatrix} \tag{2.2}$$

$$\kappa_{ik} = \begin{pmatrix} \kappa_{11} & 0 & 0 \\ 0 & \kappa_{11} & 0 \\ 0 & 0 & \kappa_{33} \end{pmatrix} \tag{2.3}$$

The compatibility equation is a geometrical constraint that must be satisfied by strain ϵ_{ij}

$$e_{ilm}e_{jpq}\frac{\partial^2 \epsilon_{mp}}{\partial x_l \partial x_q} = 0 \tag{3}$$

In eq 3 the indices are in the normal definition and Nye notation is not used. e_{ilm} and e_{jpq} are Levi−Civita antisymmetric tensors. For simplicity of the derivation, we assume that the NW bending is small.

Finally, by assuming no free charge $\rho_e^{(b)}$ in the nanowire, the Gauss equation must be satisfied

$$\nabla \cdot \vec{D} = \rho_e^{(b)} = 0 \tag{4}$$

1.2. Theory for the First Three Orders of Electromechanical Coupling. Equations 1−4 along with appropriate boundary conditions give a complete description of a static piezoelectric system. However, the solution of these equations is rather complex, and analytical solution does not exist in many cases. Even for a two-dimensional (2D) system, the solution would entail a partial differential equation of order 6.[16] In order to derive an approximate solution of the equations, we apply a perturbation expansion of the linear equations to simplify the analytical solution. Then, we will examine the accuracy of the perturbation theory in reference to the exact results calculated by the finite element method.

In order to derive the piezoelectric potential distributed in the NW for the different orders of electromechanical

coupled effect, we now introduce a perturbation parameter λ in the constitutive equations by defining $\tilde{e}_{kp} = \lambda e_{kp}$, which is introduced to trace the magnitudes of contributions made by different orders of effects in building the total potential. Consider a virtue material with linear elastic constant c_{pq}, dielectric constant κ_{ik}, and piezoelectric coefficient $\tilde{e}_{kp}$. When $\lambda = 1$, this virtue material becomes the realistic ZnO. When $\lambda = 0$, it corresponds to a situation of no coupling between mechanical field and electric field. For virtue materials with λ between 0 and 1, the mechanical field and electric field are both functions of parameter λ, which can be written in an expansion form

$$\begin{cases} \sigma_p(\lambda) = \sum_{n=0}^{\infty} \lambda^n \sigma_p^{(n)} \\ \epsilon_q(\lambda) = \sum_{n=0}^{\infty} \lambda^n \epsilon_q^{(n)} \\ E_k(\lambda) = \sum_{n=0}^{\infty} \lambda^n E_k^{(n)} \\ D_i(\lambda) = \sum_{n=0}^{\infty} \lambda^n D_i^{(n)} \end{cases} \tag{5}$$

where the superscript (n) represents the orders of perturbation results. By substituting eq 5 into eq 2 for a virtue material with piezoelectric coefficient $\tilde{e}_{kp}$, and comparing the terms in the equations that have the same order of λ, the first three orders of perturbation equations are given as follows:

zeroth order:

$$\begin{cases} \sigma_p^{(0)} = c_{pq}\epsilon_q^{(0)} \\ D_i^{(0)} = \kappa_{ik}E_k^{(0)} \end{cases} \tag{6}$$

first order:

$$\begin{cases} \sigma_p^{(1)} = c_{pq}\epsilon_q^{(1)} - e_{kp}E_k^{(0)} \\ D_i^{(1)} = e_{kq}\epsilon_q^{(0)} + \kappa_{ik}E_k^{(1)} \end{cases} \tag{7}$$

second order:

$$\begin{cases} \sigma_p^{(2)} = c_{pq}\epsilon_q^{(2)} - e_{kp}E_k^{(1)} \\ D_i^{(2)} = e_{kq}\epsilon_q^{(1)} + \kappa_{ik}E_k^{(2)} \end{cases} \tag{8}$$

For eqs 1, 3, and 4, since there is no explicit coupling, no decoupling process is needed while seeking perturbation solution.

We now consider the solutions of the first three orders. For the zeroth order (eq 6), the solution is for a bent nanowire without piezoelectric effect, which means there is no electric field even with the presence of elastic strain. For the case of ZnO NW, it normally grows with its *c*-axis parallel to the growth direction. The ±(0001) surfaces at the top and bottom end of the NW are terminated by Zn^{2+} and O^{2-} ions, respectively. The electric field due to spontaneous polarization arising from polar charges on the ±(0001) surface can be ignored for the following two reasons. First, since the NW has a large aspect ratio, the polar charges on the ±(0001) polar surfaces, which are the top and bottom ends of the NW in most of the cases, can be viewed as two point charges. Thus they do not introduce an appreciable intrinsic field inside of the NW. Second, the polar charges at the bottom end of the NW are neutralized by the conductive electrode, while the ones at the top of the NW may be neutralized by surface adsorbed foreign molecules while exposed to air. Furthermore, even if the polar charges at the top end introduce a static potential, it will not contribute to the power generated but shift the potential baseline by a constant value, which goes to the background signal, because the polar charges are present and remain constant regardless the degree of NW bending. Therefore, we can take $E_k^{(0)} = 0$, $D_i^{(0)} = 0$. Consequently, from eqs 7 and 8, we have $\sigma_p^{(1)} = 0$, $\epsilon_p^{(1)} = 0$, $D_p^{(2)} = 0$, $E_p^{(2)} = 0$. Equations 6−7 thus become

zeroth order:

$$\sigma_p^{(0)} = c_{pq}\epsilon_q^{(0)} \tag{9}$$

first order:

$$D_i^{(1)} = e_{kq}\epsilon_q^{(0)} + \kappa_{ik}E_k^{(1)} \tag{10}$$

second order:

$$\sigma_p^{(2)} = c_{pq}\epsilon_q^{(2)} - e_{kp}E_k^{(1)} \tag{11}$$

The physical meaning of these equations can be explained as follows. Under the different orders of approximation, these equations correspond to the decoupling and coupling between the electric field and mechanical deformation: the zeroth order solution is purely mechanical deformation without piezoelectricity; the first order is the result of direct piezoelectric effect that strain−stress generates an electric field in the NW; and the second order shows up the first feedback (or coupling) of the piezoelectric field to the strain in the material.

In our case as for nanowires bent by AFM tip, the mechanical deformation behavior of the material is almost unaffected by piezoelectric field in the NW. Therefore, as for the calculation of piezoelectric potential in the nanowire, the first-order approximation may be sufficient. The accuracy of this approximation will be examined in reference to full numerical solutions of the coupled eqs 1−4.

1.3. Analytical Solution under the Saint−Venant Approximation. To simplify the analytical solution, we assume that the nanowire has a cylindrical shape with a uniform cross section of diameter *2a* and length *l*. To further simplify the derivation, we approximate the material elastic constants by an isotropic elastic modulus with Young's modulus *E* and Poisson ratio *ν*. This has been found to be an excellent approximation for ZnO (see discussion in section 3). For the convenience of our calculation, we define $a_{pq}^{\text{isotropic}}$ to be the inverse of matrix $c_{pq}^{\text{isotropic}}$. The strain and stress relation is given by

$$\begin{pmatrix}\epsilon_{xx}^{(0)}\\ \epsilon_{yy}^{(0)}\\ \epsilon_{zz}^{(0)}\\ 2\epsilon_{yz}^{(0)}\\ 2\epsilon_{zx}^{(0)}\\ 2\epsilon_{xy}^{(0)}\end{pmatrix} = \sum_q a_{pq}^{\text{isotropic}}\sigma_q^{(0)} = \frac{1}{E}\begin{pmatrix}1 & -\nu & -\nu & 0 & 0 & 0\\ -\nu & 1 & -\nu & 0 & 0 & 0\\ -\nu & -\nu & 1 & 0 & 0 & 0\\ 0 & 0 & 0 & 2(1+\nu) & 0 & 0\\ 0 & 0 & 0 & 0 & 2(1+\nu) & 0\\ 0 & 0 & 0 & 0 & 0 & 2(1+\nu)\end{pmatrix}\begin{pmatrix}\sigma_{xx}^{(0)}\\ \sigma_{yy}^{(0)}\\ \sigma_{zz}^{(0)}\\ \sigma_{yz}^{(0)}\\ \sigma_{zx}^{(0)}\\ \sigma_{xy}^{(0)}\end{pmatrix} \quad (12)$$

In the configuration of the nanogenerator, the root end of the nanowire is affixed to a conductive substrate, while the top end is pushed by a lateral force f_y. We assume that the force f_y is applied uniformly on the top surface so that there is no effective torque that twists the nanowire. By Saint−Venant theory of bending,[17] the stress induced in the nanowire is given by

$$\sigma_{xz}^{(0)} = -\frac{f_y}{4I_{xx}}\frac{1+2\nu}{1+\nu}xy \quad (13.1)$$

$$\sigma_{yz}^{(0)} = \frac{f_y}{I_{xx}}\frac{3+2\nu}{8(1+\nu)}\left[a^2 - y^2 - \frac{1-2\nu}{3+2\nu}x^2\right] \quad (13.2)$$

$$\sigma_{zz}^{(0)} = -\frac{f_y}{I_{xx}}y(l-z) \quad (13.3)$$

$$\sigma_{xx}^{(0)} = \sigma_{xy}^{(0)} = \sigma_{yy}^{(0)} = 0 \quad (13.4)$$

where

$$I_{xx} = I_{yy} = \frac{\pi}{4}a^4$$

Equation 13 is the zeroth order mechanical solution to eqs 1, 3, and 12. Because the Saint−Venant principle is used to simplify the boundary condition, solution eq 13 is valid only for regions far away from the affixed end of the nanowire. Here by "far away" we mean a distance large enough in comparison to the NW diameter. Later, full numerical calculation shows that it would be safe to use eq 13 when the distance from the substrate is larger than twice the NW diameter.

Equations 4 and 10 give the direct piezoelectric behavior. By defining a remnant displacement $\vec{D}^{\mathrm{R}}$ as

$$\vec{D}^{\mathrm{R}} = e_{kq}\epsilon_q^{(0)}\hat{i}_k \quad (14)$$

we have

$$\frac{\partial}{\partial x_i}(D_i^{\mathrm{R}} + \kappa_{ik}E_k^{(1)}) = 0 \quad (15)$$

From eqs 14, 13, 12, and 2.2, the remnant displacement is

$$\vec{D}^{\mathrm{R}} = \begin{pmatrix}-\frac{f_y}{I_{xx}E}\left(\frac{1}{2}+\nu\right)e_{15}xy\\ \frac{f_y}{I_{xx}E}\left(\frac{3}{4}+\frac{\nu}{2}\right)e_{15}\left(a^2 - y^2 - \frac{1-2\nu}{3+2\nu}x^2\right)\\ \frac{f_y}{I_{xx}E}(2\nu e_{31} - e_{33})y(l-z)\end{pmatrix} \quad (16)$$

It should be noted that it is the divergence of $\vec{D}^{\mathrm{R}}$ rather than $\vec{D}^{\mathrm{R}}$ itself that induces $E_k^{(1)}$. If we simply assume $E_k^{(1)} = (\kappa_{ik})^{-1}D_i^{\mathrm{R}}$, we would arrive at an absurd electric field with nonzero curl. Instead, by defining a remnant body charge

$$\rho^{\mathrm{R}} = -\nabla\cdot\vec{D}^{\mathrm{R}} \quad (17)$$

and remnant surface charge

$$\Sigma^{\mathrm{R}} = -\vec{n}\cdot(0 - \vec{D}^{\mathrm{R}}) = \vec{n}\cdot\vec{D}^{\mathrm{R}} \quad (18)$$

Equation 15 will be transformed into an elementary electrostatic problem with the Poisson equation

$$\nabla\cdot(\kappa_{ik}E_k^{(1)}\hat{i}_i) = \rho^{\mathrm{R}} \quad (19)$$

with charge given by eq 18 on the cylindrical surface of the nanowire. From eqs 17 and 16, we have

$$\rho^{\mathrm{R}} = \frac{f_y}{I_{xx}E}[2(1+\nu)e_{15} + 2\nu e_{31} - e_{33}]y \quad (20)$$

$$\Sigma^{\mathrm{R}} = 0 \quad (21)$$

It is very important to note that, in eqs 20 and 21, the remnant charge is independent of vertical height z. Therefore, electric potential $\varphi = \varphi(x,y) = \varphi(r,\theta)$ (in cylindrical coordinates) is also independent of z. (We will drop the superscript $^{(1)}$ for the first order approximation for simplicity from here.) Physically, it suggests that the potential is uniform along the z direction except for regions very close to the ends of the nanowire. This means that the nanowire is approximately like a "parallel plate capacitor", just like we assumed for nanopiezotronics.[5,6]

Noting that $\kappa_{11} = \kappa_{22} = \kappa_\perp$, the solution of eqs 19, 20, and 21 is

$$\varphi = \begin{cases}\frac{1}{8\kappa_\perp}\frac{f_y}{I_{xx}E}[2(1+\nu)e_{15} + 2\nu e_{31} - e_{33}]\left[\frac{\kappa_0+3\kappa_\perp}{\kappa_0+\kappa_\perp}\frac{r}{a} - \frac{r^3}{a^3}\right]a^3\sin\theta, & r < a\\ \frac{1}{8\kappa_\perp}\frac{f_y}{I_{xx}E}[2(1+\nu)e_{15} + 2\nu e_{31} - e_{33}]\left[\frac{2\kappa_\perp}{\kappa_0+\kappa_\perp}\frac{a}{r}\right]a^3\sin\theta, & r \geq a\end{cases} \quad (22)$$

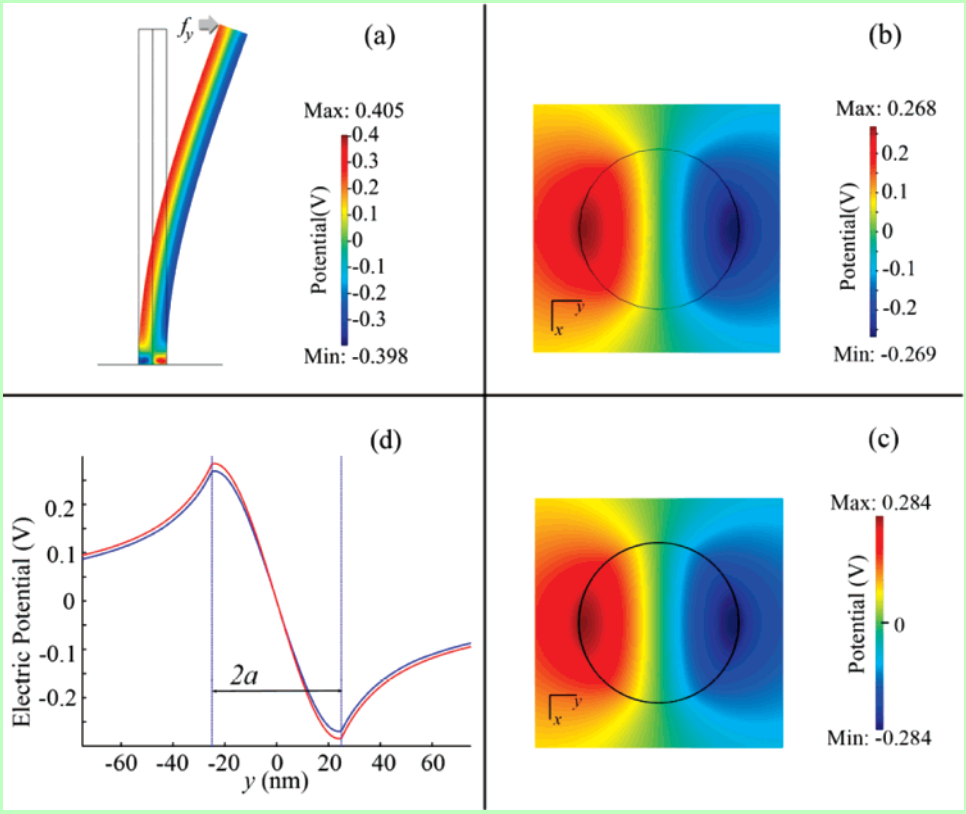

Figure 2. Potential distribution for a ZnO nanowire with $d = 50$ nm and $l = 600$ nm at a lateral bending force of 80 nN. (a) and (b) are side and top cross-sectional (at $z_0 = 300$ nm) output of the piezoelectric potential in the NW given by finite element calculation using fully coupled eqs 1−4, respectively, while (c) is the cross-sectional output of the piezoelectric potential given by analytical eq 22. The maximum potential in (b) is smaller than that in (a), because here the potential in the bottom reverse region is larger than that in upper "parallel-plate capacitor" regions. (d) gives a comparison of the line scan profiles from both (b) and (c) (blue is for full FEM, red is for eq 22) to show the accuracy of eq 22 and the approximations used for deriving it.

where κ_0 is the permittivity in vacuum. Equation 22 is the potential inside and outside the NW.

From eq 22, we have the maximum potential at the surface ($r = a$) of the NW at the tensile (T) side ($\theta = -90°$) and the compressive (C) side ($\theta = 90°$), respectively, being

$$\varphi_{\max}^{(T,C)} = \pm \frac{1}{\pi} \frac{1}{\kappa_0 + \kappa_\perp} \frac{f_y}{E} [e_{33} - 2(1+\nu)e_{15} - 2\nu e_{31}] \frac{1}{a} \quad (23)$$

By elementary elastic theory, under small deflection, the lateral force f_y is related to the maximum deflection of the NW tip $v_{\max} = v\ (z = l)$ by[18]

$$v_{\max} = \frac{f_y l^3}{3EI_{xx}} \quad (24)$$

Thus the maximum potential at the surface of the NW is

$$\varphi_{\max}^{(T,C)} = \pm \frac{3}{4(\kappa_0 + \kappa_\perp)} [e_{33} - 2(1+\nu)e_{15} - 2\nu e_{31}] \frac{a^3}{l^3} v_{\max} \quad (25)$$

This means that the electrostatic potential is directly related to the aspect ratio of the NW instead of its dimensionality. For a NW with a fixed aspect ratio, the piezoelectric potential is proportional to the maximum deflection at the tip.

2. Numerical Results and Discussion. As presented in section 1.3, we approximately represent the anisotropic elastic constant c_{pq} by an isotropic one $c_{pq}^{\text{isotropic}} = (a_{pq}^{\text{isotropic}})^{-1}$, which corresponds to modulus E and Poisson ratio ν. To examine the validity of this approximation, we define the error introduced by this approximation by

$$\left|\frac{\Delta c}{c}\right|^2 = \frac{\sum_{p,q} (c_{pq} - c_{pq}^{\text{isotropic}})^2}{\sum_{p,q} c_{pq}^{\ 2}}$$

For bulk ZnO, we have $c_{11} = 207$ GPa, $c_{12} = 117.7$ GPa, $c_{13} = 106.1$ GPa, $c_{33} = 209.5$ GPa, $c_{44} = 44.8$ GPa, and $c_{55} = 44.6$ GPa,[19] the approximating constants are $E = 129.0$ GPa and $\nu = 0.349$, with a minimized error of $\sqrt{|\Delta c/c|^2} = 3.27\%$. Therefore, our approximation is excellent. The relative dielectric constants are $\kappa_\perp^r = 7.77$ and $\kappa_{||}^r = 8.91$ for bulk ZnO,[20] and the piezoelectric constants are $e_{31} = -0.51 C/m^2$, $e_{33} = 1.22 C/m^2$, and $e_{15} = -0.45 C/m^2$ measured for film.[21] These parameters will be used in our numerical calculation.

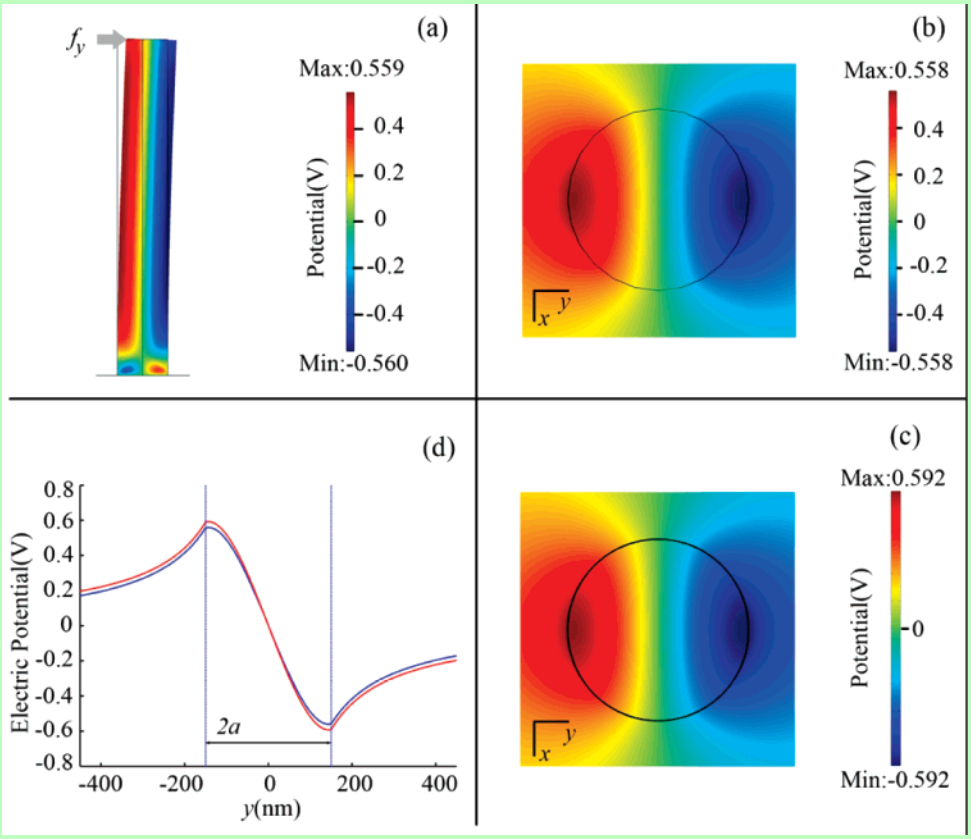

Figure 3. Potential distribution for a nanowire with $d = 300$ nm and $l = 2$ μm at a lateral bending force of 1000 nN. (a) and (b) are side and top cross-sectional (at $z_0 = 1$ μm) output of the piezoelectric potential in the NW given by finite element calculation using fully coupled eqs 1−4, respectively, while (c) is the cross-sectional output of the piezoelectric potential given by analytical eq 22. The maximum potential in (b) is almost the same as that in (a). (d) gives a comparison of the line scan profiles from both (b) and (c) (blue is for full FEM, red is for eq 22) to show the accuracy of eq 22 and the approximations used for deriving it.

We conducted the calculation based on eq 22 for two configurations: the first one is a *c*-axis vertically aligned ZnO nanowire with smaller diameter grown by vapor−liquid−solid process; the second is a large size ZnO nanowire typically grown by chemical approach. In both cases, the wires are well fixed on the substrate and pushed laterally by an AFM tip at the top.

In the first case, the wire diameter is $d = 50$ nm, length is $l = 600$ nm, and lateral force applied by AFM tip is 80 nN. To further confirm the validity of omitting the higher order terms in our analytical derivation, we performed a finite element method (FEM) calculation for a fully coupled electromechanical system using eqs 1−4 with for a simplified medium of isotropic elastic modulus tensor and with cylindrical geometry. The boundary condition assumed is that the bottom end of the NW is affixed. ZnO was considered as a dielectric medium. Parts a and b of Figure 2 are the potential distributions calculated by full FEM in the bent NW as viewed from side and in cross section, respectively, clearly presenting the "parallel plate capacitor" model of the piezoelectric potential except at the bottom. As for the nanogenerator and nanopiezotronics, only the potential distribution in the upper body of the NW matters. By use of the analytical eq 22, the calculated potential distribution across the NW cross section for a lateral defection of 145 nm (produced by 80 nN deflection force) is presented in Figure 2c, with the two side surfaces having ±0.28 V piezoelectric potential, respectively. Again we emphasize that, in eq 22, the potential is independent of z_0 except near the top and the bottom.

To compare the identity of the FEM result with the analytical result, a line scan was made across the output of the cross-section potential along the symmetry line following the lateral deflection direction, and the results are directly compared in Figure 2d. It is rather astonishing that the difference is smaller than 6%, unambiguously proving the accuracy of our analytical solution.

As mentioned before, eq 22 is based on the Saint−Venant approximation and is thus not valid in the bottom region of the NW. However, from the FEM solution we see that the bottom reverse region is small, extending only for less than twice the nanowire diameter. Therefore, eq 22 is useful even for nanowires with rather small aspect ratio. The physical consequence of the bottom reverse region needs to be further investigated, both theoretically and experimentally. For example, such a barrier could give rise to interesting effect in piezoelectric field effect transistor (PE-FET) applications.

A similar calculation has been done for a large size NW with $d = 300$ nm, length $l = 2$ μm, and a lateral force of 1000 nN. The value of pushing force is estimated based on the lateral deflection observed experimentally. Analogous to the case shown for the smaller NW in Figure 2, this large

NW gives a potential distribution of ±0.59 V across its cross section. Again, the analytical solution is within 6% of the FEM full numerical calculation, clearly proving the validity of our analytical solution. Therefore, the perturbation theory we have presented here is an excellent representation for calculating the piezoelectric potential across a NW, and the analytical results given by eqs 22−25 can be applied to quantitatively understand the experimentally measured results.

It must be pointed out that the elastic modulus and piezoelectric ceefficient used for the calculations presented here were adopted from the values measured from bulk and film. Previous experimental measurements show a reduction in elastic modulus for ZnO nanowire[22,23] and an increased piezoelectric coefficient (by 200%).[24] If these values were used in above calculations, the potential on the NW surface would be increased by a factor of 3−4.

From the calculation presented above, 0.3 V is created between the NW and the AFM tip during mechanical bending. This voltage is much higher than the thermal voltage of $k_BT/e \sim 25$ mV, and it is applied to the Schottky barrier between the NW and the tip and is responsible for driving the rectifying behavior of the Schottky barrier.

In practice, the received voltage is in the order of 10 mV, much lower than that calculated theoretically for the following reasons. First, a single NW based nanogenerator (see Figure 1) can be simplified as a voltage source V_{nw}, which is created by the piezoelectric effect of the NW when subjected to mechanical deformation, a contact resistance R_s between the tip and the NW, and an inner resistance R_{nw} of the NW. Since the ZnO NW was a bare NW without a catalyst particle at the tip, the contact resistance (R_c) can be very large due to the small contact area between the metal tip and the edge of the NW tip. Therefore, the voltage that drove the Schottky diode (V_{nw}) was largely consumed at the contacted resistance, and only a small portion was received as the output. Second, the capacitance of the nanogenerator system (∼1 pF) is much larger than the capacitance of a single NW (∼fF). The large system capacitance consumes most of the charges produced by the NW, and the large system capacitance results in low voltage output, but the output current should not be affected.

In summery, under a small deflection approximation, we have applied the perturbation theory to analytically calculate the piezoelectric potential distribution in a nanowire as pushed by a lateral force at the tip. The analytical solution given under the first-order approximation produces a result that is within 6% from the full numerical calculated result using a finite element method, clearly establishing the accuracy and validity of our theory. The calculation shows that the piezoelectric potential in the NW almost does not depend on the *z*-coordination along the NW unless very close to the two ends, meaning that the NW can be approximately taken as a "parallel plated capacitor". This is entirely consistent to the model established for nanopiezotronics, in which the potential drop across the nanowire serves as the gate voltage for the PE-FET. The maximum potential at the surface of the NW is directly proportional to the lateral displacement of the NW and inversely proportional to the cube of length-to-diameter aspect ratio of the NW. The magnitude of piezoelectric potential for a NW of diameter 50 nm and length 600 nm is ∼0.3 V. This voltage is high enough to drive the metal−semiconductor Schottky diode at the interface between AFM tip and the ZnO NW, as assumed in our original mechanism for the nanogenerator.

Acknowledgment. Thanks to NSF and Emory Georgia Tech CCNE (NIH) for support. Thanks to Dr. Xudong Wang and Jinhui Song for stimulating discussions.

References

(1) Wang, Z. L.; Song, J. H. *Science* **2006**, *312*, 242−246.
(2) Gao, P. X.; Song, J. H.; Liu, J.; Wang, Z. L. *Adv. Mater.* **2007**, *19*, 67−72.
(3) Song, J. H.; Zhou, J.; Wang, Z. L. *Nano Lett.* **2006**, *6*, 1656−1662.
(4) Wang, X. D.; Song, J. H.; Liu, J.; Wang, Z. L. *Science* **2007**, *316*, 102−105.
(5) Wang, Z. L. *Mater. Today* **2007**, *10*, 20−28.
(6) Wang, Z. L. *Adv. Mater.* **2007**, *19*, 889−992.
(7) Wang, X. D.; Zhou, J.; Song, J. H.; Liu, J.; Xu, N. S.; Wang, Z. L. *Nano Lett.* **2006**, *6*, 2768−2772.
(8) He, J. H.; Hsin, C. L.; Chen, L. J.; Wang, Z. L. *Adv. Mater.* **2007**, *19*, 781−784.
(9) Lao, C. S.; Kuang, Q.; Wang, Z. L.; Park, M. C.; Deng, Y. L. *Appl. Phys. Letts.* **2007**, *90*, 262107.
(10) Xiang, H. J.; Yang, J. L.; Hou, J. G.; Zhu, Q. S. *Appl. Phys. Lett.* **2006**, *89*, 223111.
(11) Tu, Z. C.; Hu, X. *Phys. Rev. B* **2006**, *74*, 035434.
(12) A J Kulkarni, M. Z. a. F. J. K. *Nanotechnology* **2005**, *16*, 2749−2756.
(13) Michalski, P. J.; Sai, N.; Mele, E. J. *Phys. Rev. Lett.* **2005**, *95* (11), 116803.
(14) Wang, Z. L.; Kong, X. Y.; Ding, Y.; Gao, P. X.; Hughes, W. L.; Yang, R. S.; Zhang, Y. S. *Adv. Funct. Mater.* **2004**, *14* (10), 943−956.
(15) Nye, J. F. *Physical Properties of Crystals*; Oxford University Press: Oxford, 1957.
(16) Qin, Q.-H. *Fracture Mechanics of Piezoelectric Materials*; WIT Press: Southampton, U.K., 2001.
(17) Soutas-Little, R. W. *Elasticity*; Dover Publications: Mineola, NY, 1999.
(18) Landau, L. D.; Lifshiëtìs, E. M. *Theory of elasticity*; Pergamon Press, Addison-Wesley Publishing Co.: London and Reading, MA, 1959.
(19) Kobiakov, I. B. *Solid State Commun.* **1980**, *35*, 305−310.
(20) Ashkenov, N.; Mbenkum, B. N.; Bundesmann, C.; Riede, V.; Lorenz, M.; Spemann, D.; Kaidashev, E. M.; Kasic, A.; Schubert, M.; Grundmann, M.; Wagner, G.; Neumann, H.; Darakchieva, V.; Arwin, H.; Monemar, B. *J. Appl. Phys.* **2003**, *93* (1), 126−133.
(21) Carlotti, G.; Socino, G.; Petri, A.; Verona, E. *Appl. Phys. Lett.* **1987**, *51* (23), 1889−1891.
(22) Song, J. H.; Wang, X. D.; Riedo, E.; Wang, Z. L. *Nano Lett.* **2005**, *5*, 1954−1958.
(23) Chen, C. Q.; Shi, Y.; Zhang, Y. S.; Zhu, J.; Yan, Y. J. *Phys. Rev. Lett.* **2006**, *96*, 075505.
(24) Zhao, M. H.; Wang, Z. L.; Mao, S. X. *Nano Lett.* **2004**, *4*, 587−590.

NL071310J